Research Article – Vol. 01, Issue 01, No. 06

Bilji publication

Advanced in Engineering and Intelligence Systems

Journal Web Page: https://aeis.bilijipub.com

A novel hybrid radial basis function method for predicting the fresh and hardened properties of self-compacting concrete

Zhangabay Nurlan[1,*]

[1] *Department of industrial, civil and road building, м.auezov south Kazakhstan state university*

Highlights

- Novel hybrid radial basis function (RBFNN) networks were developed
- Two optimization algorithms named ant-lion optimization (ALO) and biogeography optimization (BBO) applied to RBFNN
- BBO-RBFNN and ALO-RBFNN were suggested for predicting the fresh and hardened properties of self-compacting concrete
- L-box test, V-funnel test, and slump flow in the fresh phase of concrete, and compressive strength in the hardened phase
- Regarding D flow, L-box, V-funnel, and CS, the results of ALO-RBFNN were better than BBO-RBFNN and literature.

Article Info

Received: 19 January 2022
Received in revised: 04 April 2022
Accepted: 04 April 2022
Available online: 16 April 2022

Keywords

Self-compacting concrete
Fly ash
Rheological properties
Compressive strength
Radial basis function neural network

Abstract

It is observed from the published literature that there were so limited studies concentrating on predicting both fresh and hardened properties of self-compacting concrete (SCC). Hence, it is tried to develop models for predicting the fresh and hardened properties of SCC by the optimized radial basis function neural network (RBFNN) method. The RBFNN method's key parameters are optimized using ant-lion optimization (ALO) and biogeography optimization (BBO) algorithms. The considered properties of SCC in the fresh phase are the L-box test, V-funnel test, slump flow, and compressive strength (CS) in the hardened phase. Results demonstrate powerful potential in the learning section as well as approximating in the testing phase. It means that the correlation between observed and predicted properties of SCC from hybrid models is acceptable so that it represents high accuracy in the training and approximating process. Regarding D flow, L-box, V-funnel, and CS, the results of ALO-RBFNN were better than BBO-RBFNN and literature. Overall, the RBFNN model developed by ALO outperforms others, which depicts the capability of the ALO algorithm for determining the optimal parameters of the considered method.

Nomenclature

ALO	Ant lion optimizer	FA	Fly ash
B	Dosage of binder content	LB	L-box
BBO	Biogeography-based optimization	$RBFNN$	Radial basis function neural network
CAG	Coarse aggregate	SCC	Self-compacting concrete
CS	Compressive strength	SP	Superplasticizer
DF	D flow	VF	V-funnel
FAG	Fine aggregate	W/B	Water to powder ratio

1. Introduction

In 1988, in Japan, self-compacting concrete (SCC) was first extended. These days, SCC is a very effective concrete blend worldwide [1]–[6]. SCC is a kind of concrete that is able to load and flow the formatting with no exterior power. As well, it can strengthen by weight of its own [7]. The design mix initially focused on the two original criteria, with the need for the big value of better particle and urgency of high-performing water decreasing mixture. Compared to different common concrete, it needs comparatively minor

* Corresponding Author: Zhangabay Nurlan
Email: zhangabaynurlan@gmail.com

human attempts that are an added benefit. As well, it increments output level and decreases noise disorders. Many explore studies are being performed in the SCC technology zone; several of these explores suggest finer increment and continuity. Alongside of all these benefits, SCC has several minus parts. The expense of output of SCC is able to be 2-3 chances bigger than normal concrete. Hence, to lower the expense, several various mixtures like metakaolin, fly ash (FA), limestone filler, ground-granulated blast-furnace slag, and ground clay bricks can be used [8]. These components utilized actions as a suitable replacement for Portland cement [9]–[14]. To extend SCC, three criteria must be carried out, like filling capability, passing capability, and separation resistance. Then, to meet out these needs, some test experiments are required to be carried out. Many questions occur that SCC is affordable and expense-effective.

Nowadays, the successful applications of the artificial neural network in different civil engineering fields have been reported adapted from experimental results [15]–[18]. This usage is widely-expanded in the concrete industry to predict different properties of concrete. Oxcan et al. [19] carried out comparative research considering two methods, with ANN and fuzzy logic, to predict the compressive strength of silica fume concrete. For analogous usages, several of the different scholars as well as suggested appropriate samples inspired by Fuzzy and adaptive neuro-fuzzy inference system (ANFIS) to compute the compressive strength [20]–[23]. Newly, Sonebi et al. [24] studied the new attributes of SCC utilizing SVR proceed. The outcome was affirmative and incentive that presents finer filling and passing capability. Various scholars performed analogous study work to forecast the compressive strength of concrete utilizing SVR [25]–[27]. Liu [28] considered the possibility of utilizing an SVM sample to specify autogenous shrinkage of concrete admixtures. Reciprocally, Yang [29] conducted empirical research on corroded reinforced concrete. Other papers are also developed different models to predict the properties of SCC, such as the ANN technique [20], M5' and MARS based prediction models [30], and support vector regression approach [31] for predicting the slump flow, the L-box ratio, the V-funnel time and the compressive strength.

According to the aim of this study about using radial basis function neural network (RBFNN) as well as newly developed optimization algorithms, it is worth discussing this object [32]–[36]. The CS of SCC containing FA was predicted using hybrid biogeography-based optimization (BBO) with fuzzy RBFNN [37], [38]. The results strongly presented that the developed hybrid model has the acceptable performance to predict the CS of SCC with FA [39]. Another study focused on predicting the CS of SCC containing Class F FA using a hybrid RBFNN and firefly optimization algorithm (FOA) hybrid model. The results depict that the CS predicted by the proposed models have appropriate performance compared to the experimental results [40].

Nevertheless, most of the literature on concrete was restricted just to forecasting the hardened concrete characteristics. It is received from the published articles that there were so limited studies concentrating on predicting either fresh or hardened properties of self-compacting concrete (SCC) using the optimized RBFNN method. Hence, it is tried to develop models for predicting the fresh and hardened properties of SCC by the RBFNN method. The RBFNN method has key parameters that can be optimized with optimization algorithms, where this study aimed to determine them using ant-lion optimization (ALO) and biogeography optimization (BBO) algorithms. Experimental data records were gathered from published literature to develop the ALO-RBFNN and BBO-RBFNN models. The considered properties of SCC in the fresh phase are the L-box test, V-funnel test, slump flow, and compressive strength in the hardened phase.

2. Materials and methods

2.1.Data description

This study aimed to develop models to predict the resulting variables related to self-compacting concrete's fresh and hardened properties (SCC). Most of the published literature has been working with a limitation of assessing a single output property of concrete by using many input datasets. Hence, in the present study, four output properties of SCC named D flow, L-box, V-funnel, and compressive strength are considered to use in the prediction process. To this aim, a dataset has been made by collecting 114 SCC samples from published literature [41]–[53]. The input variables contain components of concrete: binder content (B), fly ash percentage (FA), water to binder ratio (W/B), fine aggregate (FAG), coarse aggregate (CAG), and superplasticizer dosage (SP). In this study, the dataset was divided at 70% for training data and the rest (30) for the testing phase [54]. Statistical parameters of the dataset and their histogram plots are presented in Table1 and Fig. 1.

Table 1. Statistical parameters of input and output variable

Category	Parameter	Input variable						Output variable			
		B	FA	W/B	FAG	CAG	SP	DF	LB	VF	CS
Train	Min.	370	0.0	0.26	656	590	0.74	510	0.6	2	23
	Max.	733	60	0.45	1010	935	21.84	810	1.0	19.2	86.8
	St. D.	73.4506	15.74	0.061	92.54	120.486	4.703	53.321	0.084	4.047	17.408
	Var.	5394.99	247.67	0.004	8563.65	14517.02	22.12	2843.14	0.007	16.378	303.07
	Range	363	60	0.19	354	345	21.1	300	0.4	17.2	63.8
	Skew.	0.0869	-0.288	-0.406	-0.272	-0.0644	0.677	-0.0457	-0.52	0.493	0.4955
	Kurt.	0.4472	-0.575	-1.059	-1.1257	-1.5461	0.494	0.3045	0.1314	-0.289	-0.908
Test	Min.	400	0.0	0.27	686	590	0.86	480	0.6	2.5	17
	Max.	628	60	0.45	1038	926	19.53	770	1	14.5	82.9
	St. D.	64.463	17.941	0.057	77.842	121.657	4.518	60.735	0.109	3.243	17.251
	Var.	4155.556	321.89	0.0033	6059.42	14800.36	20.411	3688.79	0.0120	10.5166	297.59
	Range	228	60	0.18	352	336	18.67	290	0.4	12	65.9
	Skew.	-0.5276	0.3895	-0.626	-0.219	0.2066	0.496	-0.1246	-0.799	0.1133	0.454
	Kurt.	-0.5108	-0.555	-1.055	-0.0220	-1.5411	0.2141	0.8255	0.1453	-1.1721	-0.526

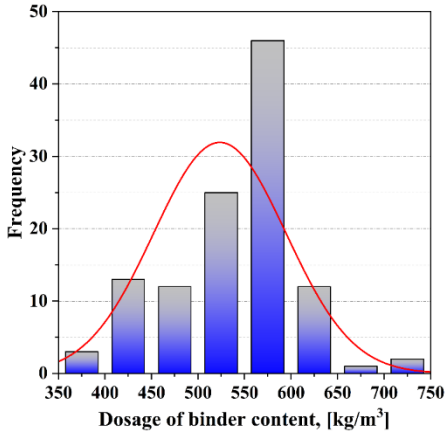

(A-1)

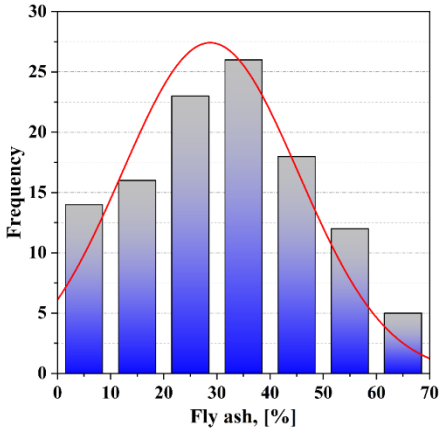

(A-2)

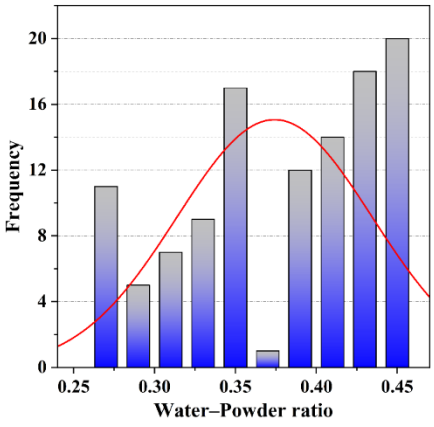

(A-3)

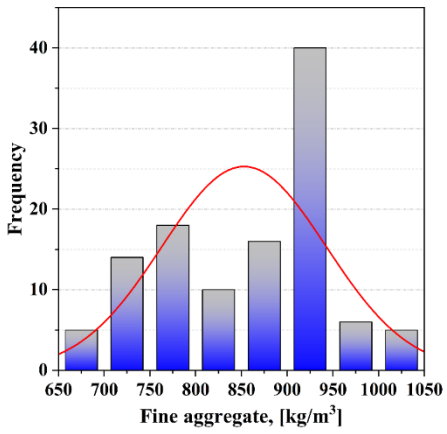

(A-4)

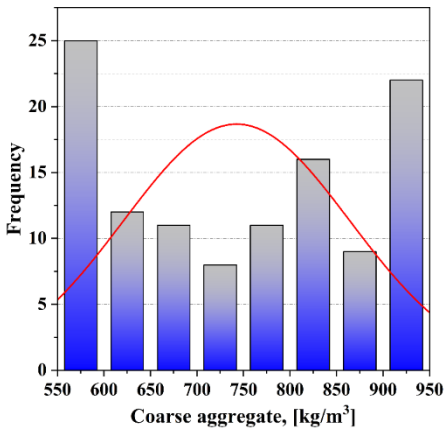

(A-5)

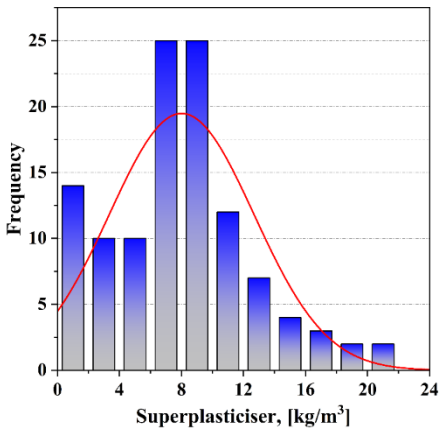

(A-6)

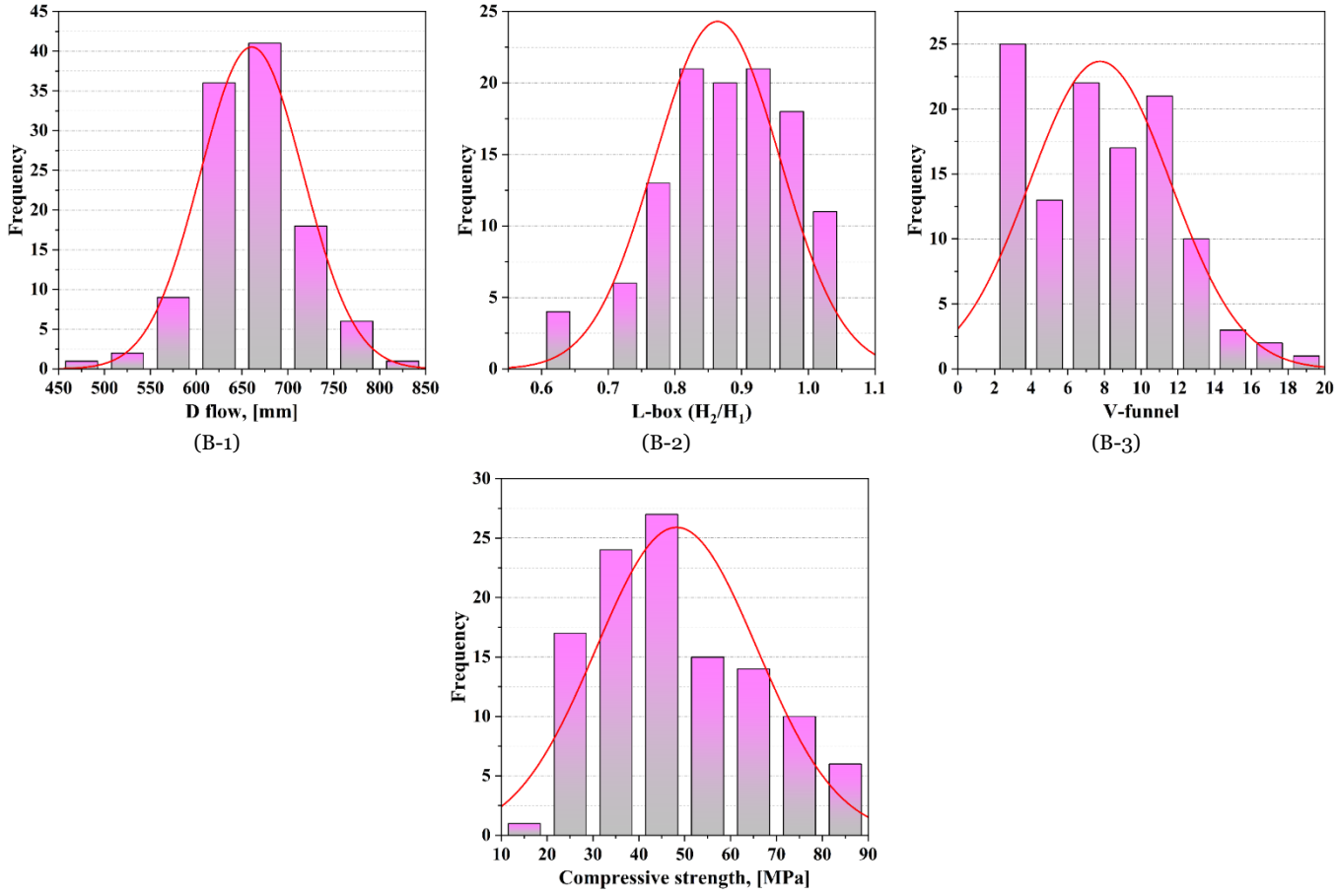

Fig. 1. The histogram plots of the input and output variables

2.2. Equality constraints

ALO swarm-based optimization method was developed by mimicking the behavior of ant lions (AL) via their life [55]. Same as other methods, this method aims to specify the most accurate fitting solution for an issue during iterations. The first locations of the lions and the hunt are accidentally adjusted in the pursuit space. The ALO flowchart is presented in Fig. 2. Steps during each iteration are: random walk of prey, trapping in holes, constructing a trap, sliding the hunt, hunting the prey, and determining the elite.

Based on Eq. 1, the movement of the brought-up ants is notified by cumulative sum (C_{sum}) [55]:

$$X(t) = [0, C_{sum}(2r(t_1)) - 1, \dots, C_{sum}(2r(t_n)) - 1] \quad (1)$$

$$r(t) = \begin{cases} 1, rand(0,1) > 0.5 \\ 0, rand(0,1) \le 0.5 \end{cases} \quad (2)$$

Where "*rand*" is a random number that is exactly divided from 0 to 1. After that, assuming X_i^t is the position of the i^{th} variable, a normalization function is applied at each iteration [55]:

$$X_i^t = \frac{(X_i^t - a_i).(d_i^t - c_i^t)}{b_i - a_i} + c_i^t \quad (3)$$

d_i^t : Maximum of the introduced variable

c_i^t : Minimum of the introduced variable

b_i : Maximum of accidental walk in the i^{th} variable

a_i : Minimum of accidental walk in the i^{th} variable

Eqs. 4-5 show the mathematical effect of the holes of AL on the random hunt walk (Fig. 3a) [55].

$$c_i^t = Antlion_j^t + c^t \quad (4)$$

$$d_i^t = Antlion_j^t + d^t \quad (5)$$

$Antlion_j^t$: the location of j^{th} AL

d^t : vectors with the maximum of variables

c^t : vectors with the minimum of variables

In the ALO method, it is assumed that one hunter traps each hunt. So, the performance of the prey assists to the lion hunting capability is a function of so-called Roulette Wheel Selection (RWS) is done herein. Considering this, the ant

lions that have bigger fitness contain a larger chance to catch better prey. Parameter I is supposed that rely on the present iteration and the number of iterations ratio. Eqs. (6-7) depicts the prey sliding to the trap mathematically (Fig. 3b). Executing this decline in the pursuit space contributes to obtaining a more suitable convergence into being optimized.

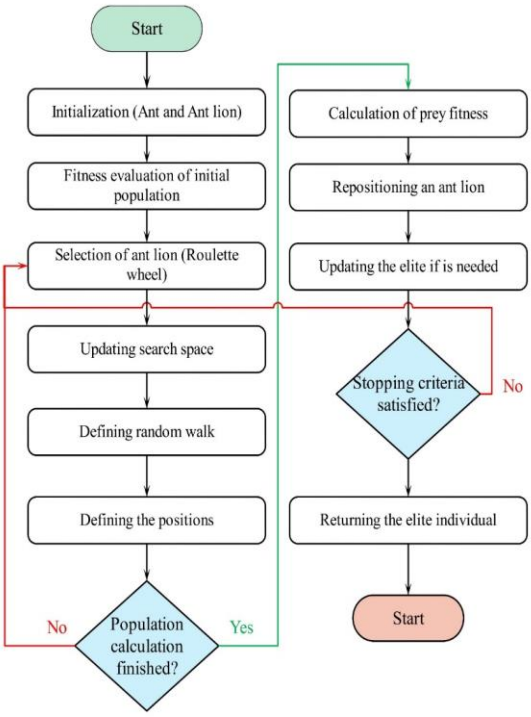

Fig. 2. The flowchart of the ALO algorithm

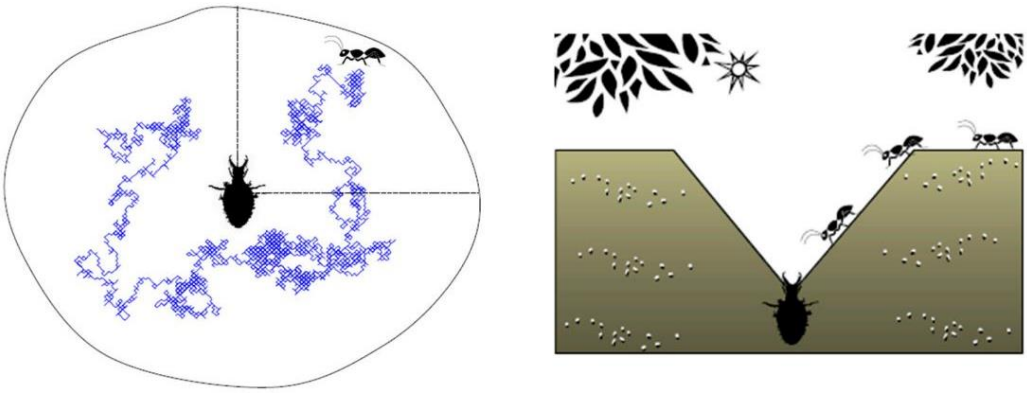

(a) **(b)**

Fig. 3. a) Random walk of the prey inside the trap, and b) hunting behavior of ant lions

$$c^t = \frac{c^t}{I} \tag{6}$$

$$d^t = \frac{d^t}{I} \tag{7}$$

Finally, hunting the prey, also AL reposition, is determined as Eq. (8) [55].

$$f(Ant_i^t) < f\left(Antlion_j^t\right) \rightarrow Antlion_j^t = Ant_i^t \tag{8}$$

After that, the clever ant lion is determined, as well the position of whole relations within the pursuit space is assumed to be affected by the position of clever number. A random walk of the hunt AL selection via the RWS is

recognized by R_A^t, and the random walk of the same hunt close to the foremost hunter is R_E^t [55]:

$$Ant_i^t = \frac{R_A^t + R_E^t}{2} \quad (9)$$

2.3. Biogeography-based optimization constraints

BBO algorithm is a metaheuristic algorithm inspired by geographical distribution, emigration, and immigration of kinds within an ecosystem [56]. In this optimization algorithm, it is supposed which an ecosystem contains a limited number of habitats. Various parameters called suitability index variables impact each habitat quality for species, containing food, climate condition, water resources, etc. habitat suitability index (HSI) is an index to present the quality of each habitat. If a habitat is full or has a big HSI, the species tend to emigrate from this habitat and immigrate to the small value of HSI. Each living place supplied a feasible solution, and its SI is the decision variable (DVs). During the optimization process, the solutions with smaller values for objective have larger values of habitat suitability indexes. In this algorithm, two operators named "migration" and "mutation" are utilized, in which migration operator is applied to find the vicinity of the existing answers, and mutation one is used to explore the new answers and assist the exploration.

For habitats with the size of HS, the habitats are listed from their cost function values. The suitability of the i^{th} habitat (HSI_i) in the sorted generation is specified as Eq. (10) [56].

$$HSI_i = -i + HS + 1 \quad (10)$$

The emigration (μ_i) and immigration (λ_i) values are calculated as follows:

$$\mu_i = \frac{HSI_i}{HS} \quad (11)$$

$$\lambda_i = 1 - \frac{HSI_i}{HS} \quad (12)$$

The given Fig. 4 shows the migration process of the BBO. Here, the highest value of emigration and immigration speed is supposed to be 1. Migration from the j^{th} decision variable of r^{th} habitat to the decision variable of i^{th} habitat is [56]:

$$DV_j^k = \alpha DV_j^i + (1-\alpha) DV_j^r \quad (13)$$

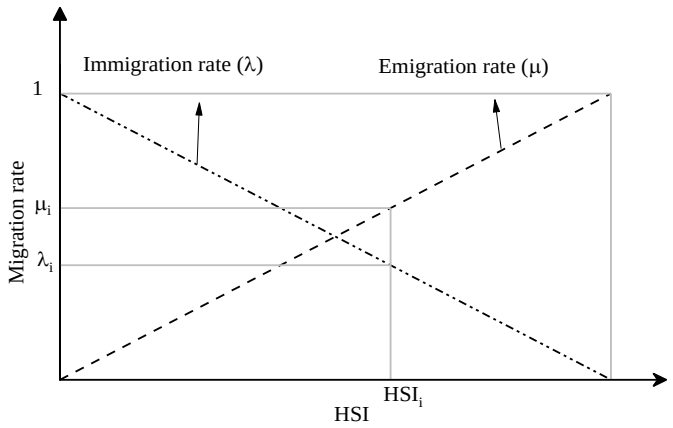

Fig. 4. Migration curve of the BBO algorithm

2.4. Hybrid radial basis function neural network

A radial base function neural network (RBFNN) is recognized as a feed-forward network containing one input, hidden, and output layer. Hence, the convergence speed rate of an RBFNN is high [57]. The input nodes transition input variables from the input layer to the hidden layer, which a Gaussian activation function shapes the hidden layer nodes. This neural network reacts to the input signals close to the center of the base function. The resulted output of the hidden layer is transmitted to the output layer, which mainly employs a simple linear function [58].

Fig. 5 represent the structure of RBFNN, in which $t_1, t_2, \dots, t_5$ are the network inputs and $\varphi_1, \varphi_2, \dots, \varphi_q$ are the center of the base function in the hidden layer. Also, $w_0, w_1, \dots, w_q$ depicts the weights in which w_0 represents the output layer weight. The Gaussian function (φ) used in this research is as Eq. (14) [57]:

$$\varphi_i = exp\left(-\frac{\|t - c_i\|}{\sigma_i^2}\right) \quad (14)$$

φ_i : Output of i^{th} node of hidden layer

c_i : Prototype center of i^{th} Gaussian function

σ : Spread rate parameter

$\|t - c_i\|$: Distance between input t and c_i

The output of an RBFNN could be presented via Eq. (15) [57]:

$$Y = W^T \varphi = \sum_{i=1}^{q} w_i \varphi(\|t - c_i\|) \quad (15)$$

The RBFNN is an adjustable technique that automatically dedicates the spread rate and the hidden layer's neuron number. Determining parameters in the efficiency of RBFNN defines the best combination of neuron numbers and spread rate. The integrated ALO-RBFNN and BBO-RBFNN methods are applied to gain the most accurate RBFNN in the present study. The ALO and

BBO algorithms determine the hidden neurons' number and the spread value to set the RBFNN structure. The highest allowable hidden neurons' number was equal to 100. Therefore, ALO-RBFNN and BBO-RBFNN try to build a superior model with suitable values for the variables mentioned above.

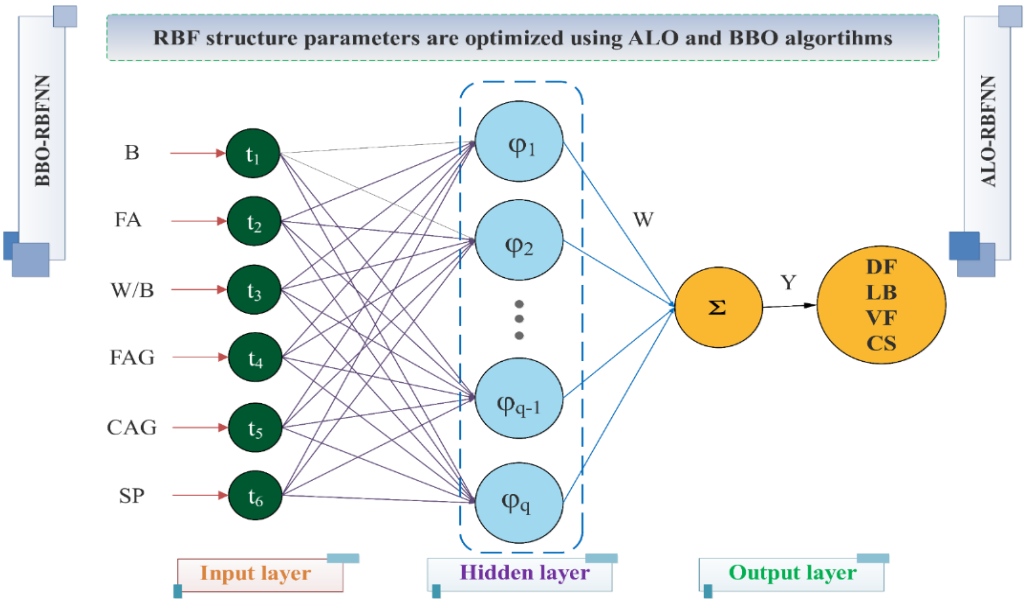

Fig. 5. Radial basis function structure

2.5. Performance evaluation indices

Different statistical performance evaluators were applied to estimate the performance of developed hybrid models for forecasting the considered properties. To this aim, the Coefficient of determination (R^2), root mean squared error (RMSE), and mean absolute error (MAE) were calculated as precision measurements (Eqs. (16-18)):

$$R^2 = \left(\frac{\sum_{p=1}^{P}(t_P - \bar{t})(y_P - \bar{y})}{\sqrt{\left[\sum_{p=1}^{P}(t_P - \bar{t})^2\right]\left[\sum_{p=1}^{P}(y_P - \bar{y})^2\right]}} \right)^2 \quad (16)$$

$$RMSE = \sqrt{\frac{1}{P}\sum_{p=1}^{P}(y_p - t_p)^2} \quad (17)$$

$$MAE = \frac{1}{P}\sum_{p=1}^{P}|y_p - t_p| \quad (18)$$

Where, y_P, t_P, $\bar{t}$, and $\bar{y}$ represent the predicted values of the P^{th} pattern, the target values of the P^{th} pattern, the averages of the target values, and the averages of the predicted values, respectively.

3. Results and discussion

The results of the RBFNN models for predicting fresh and hardened properties of SCC are supplied as follows. As mentioned above, determining the main parameters in the efficiency of RBFNN is defining the best combination of neuron numbers and spread rate. The integrated ALO-RBFNN and BBO-RBFNN methods are applied to gain the most accurate RBFNN in the present study. The optimized values of these determinative parameters for four properties of SCC (D flow, L-box, V-funnel, and CS) are presented in Table 2.

Table 2. Value of RBF parameters (continued).

Properties	RBF Parameters	ALO-RBF	BBO-RBF
D flow	Hidden neurons' number	98	83
	Spread value	2.6709	1.2504
L-box	Hidden neurons' number	98	96
	Spread value	3.91069	1.4098
V-funnel	Hidden neurons' number	99	74
	Spread value	3.8276	2.112

Compressive strength	Hidden neurons' number	93	81
	Spread value	1.439	1

Fig. 6 demonstrates powerful potential in the learning section as well as approximating in the testing phase. Comparing the measurements with those predicted by developed models are supplied in Fig. 6 for ALO-RBFNN and BBO-RBFNN, related to fresh and hardened properties of SCC. It can be seen that the proposed models have R^2 in acceptable value in the learning and testing phase. It means that the correlation between observed and predicted properties of SCC from hybrid models is acceptable so that it represents high accuracy in the training and approximating process.

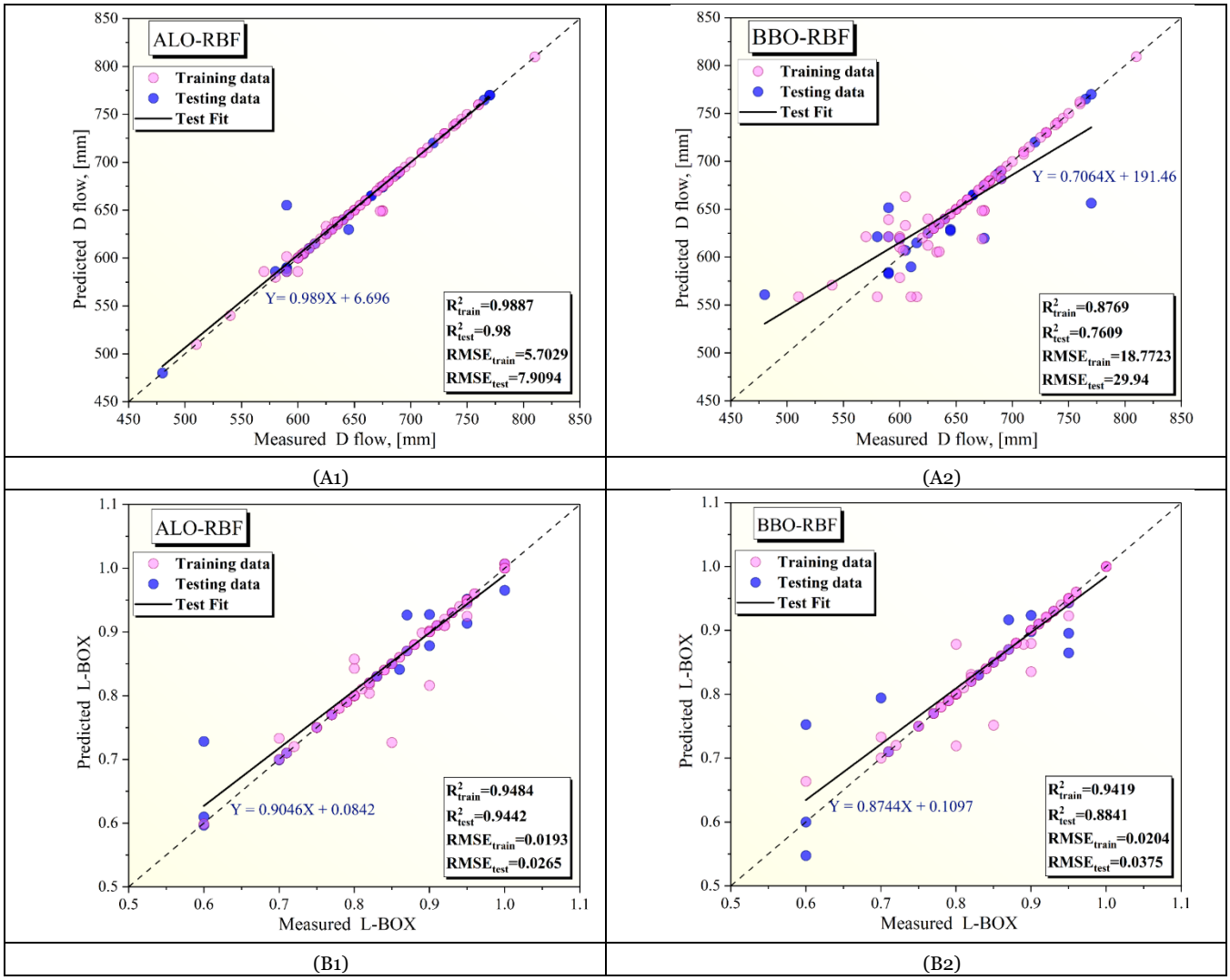

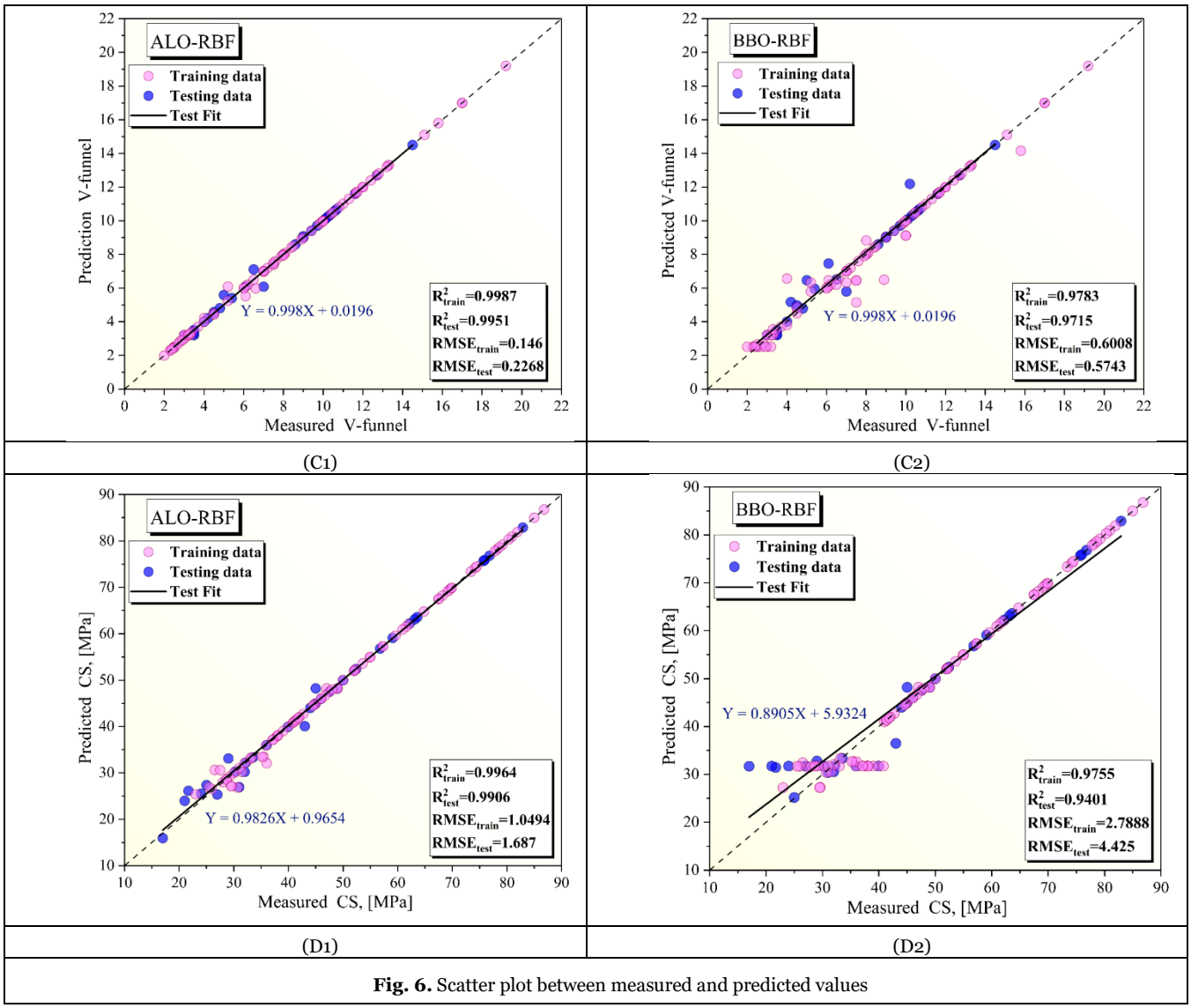

Fig. 6. Scatter plot between measured and predicted values

Besides, the results of developed models considering R^2, RMSE, and MAE values for fresh and hardened properties of SCC are supplied in Table 3. The results of the proposed models in this study have been compared with the published literature [31]. Regarding D flow, the results of ALO-RBFNN are so better than BBO-RBFNN as well as literature. For example, the RMSE value of the model by ALO in the training phase is 7.5154mm, while this value for the BBO-RBFNN model is more than twice, followed by Saha et al. (2020) at 11.67mm, and then Kaveh et al. (2018) by 36.29mm. Regarding L-box, the results of ALO-RBFNN are better than BBO-RBFNN as well as literature. For example, the RMSE value of the model by ALO in the testing phase is 0.0265, while this value for the BBO-RBFNN model is roughly less than twice, and followed by Saha et al. (2020) at 0.025, and then Kaveh et al. (2018) by 0.06. Turning to V-funnel results, the results of ALO-RBFNN are extremely better than BBO-RBFNN as well as literature. For instance, R^2 value of the model by ALO in the testing phase is 0.9951, while this value for the BBO-RBFNN model is 0.9715, followed by Saha et al. (2020) at 0.958, and then Kaveh et al. (2018) by 0.87. Finally, the result for CS also depicts the same outputs as above. Overall, the RBFNN model developed by ALO outperforms others, which depicts the capability of the ALO algorithm for determining the optimal parameters of the considered method. However, it is worth mentioning that the model developed with the BBO algorithm is also powerful.

A justifiable fit between measured values and predicted values is acquirable from the time series figures reported in Figs—7 (a-d). As can be seen, for fresh and hardened properties of SCC in both optimized RBFNN (ALO-RBFNN and BBO-RBFNN) proposed models, the estimated values indicate suitable agreement with

measured ones, expressing the workability of suggested integrated algorithms to forecast the D flow, L-box, V-funnel, and CS with high precision. According to time series figures, developed models result in the lowest variation in the properties predicting process, providing roughly accurate predictions which can be used for practical applications.

Table 3. Statistical errors of proposed SVR models

Properties	Index	Data phase	ALO-RBFNN	BBO-RBFNN	[31]	[30]
D flow	R^2	Training data	0.9802	0.8769	0.931	0.57
		Testing data	0.9771	0.7609		
	RMSE	Training data	7.5154	18.7723	11.678	36.29
		Testing data	9.2382	29.94		
	MAE	Training data	2.7258	9.1572		27.66
		Testing data	3.5702	14.1120		
L-box	R^2	Training data	0.9484	0.9419	0.91	0.56
		Testing data	0.9442	0.8841		
	RMSE	Training data	0.0193	0.0204	0.025	0.06
		Testing data	0.0265	0.0375		
	MAE	Training data	0.0055	0.0063		0.05
		Testing data	0.0104	0.0152		
V-funnel	R^2	Training data	0.9987	0.9783	0.958	0.87
		Testing data	0.9951	0.9715		
	RMSE	Training data	0.146	0.6008	0.723	1.46
		Testing data	0.2268	0.5743		
	MAE	Training data	0.0422	0.2645		1.11
		Testing data	0.0880	0.2710		
Compressive strength	R^2	Training data	0.9964	0.9755	0.955	0.93
		Testing data	0.9906	0.9401		
	RMSE	Training data	1.0494	2.7888	3.783	4.45
		Testing data	1.687	4.425		
	MAE	Training data	0.4032	1.4765		3.45
		Testing data	0.9154	2.3133		

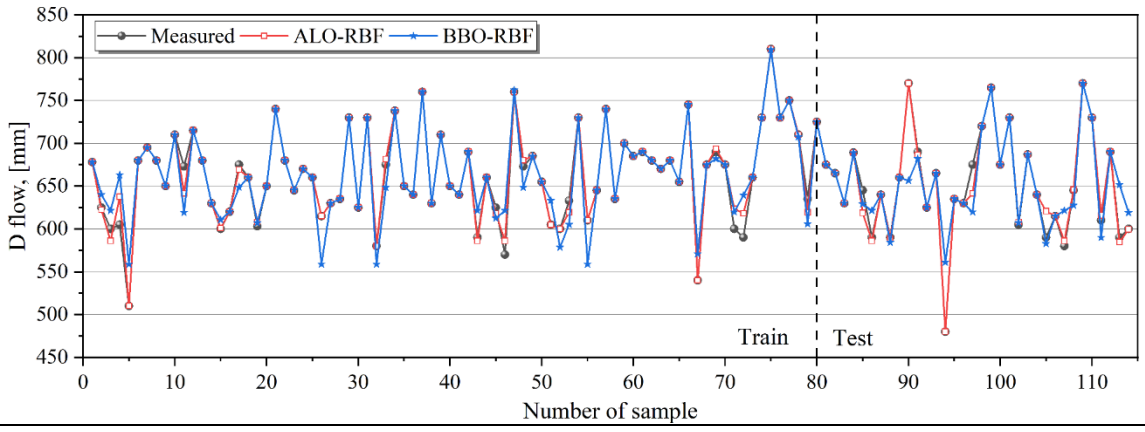

(a)

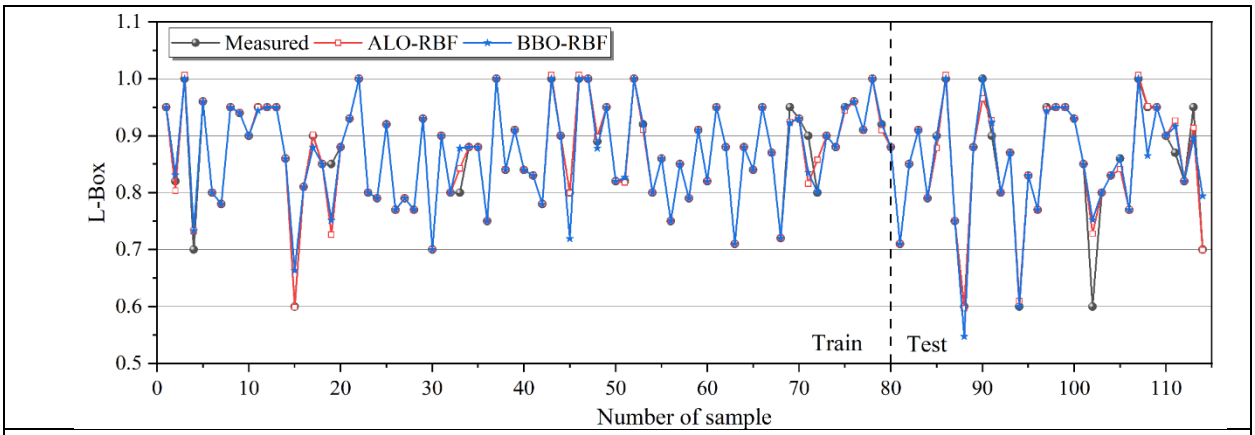

(b)

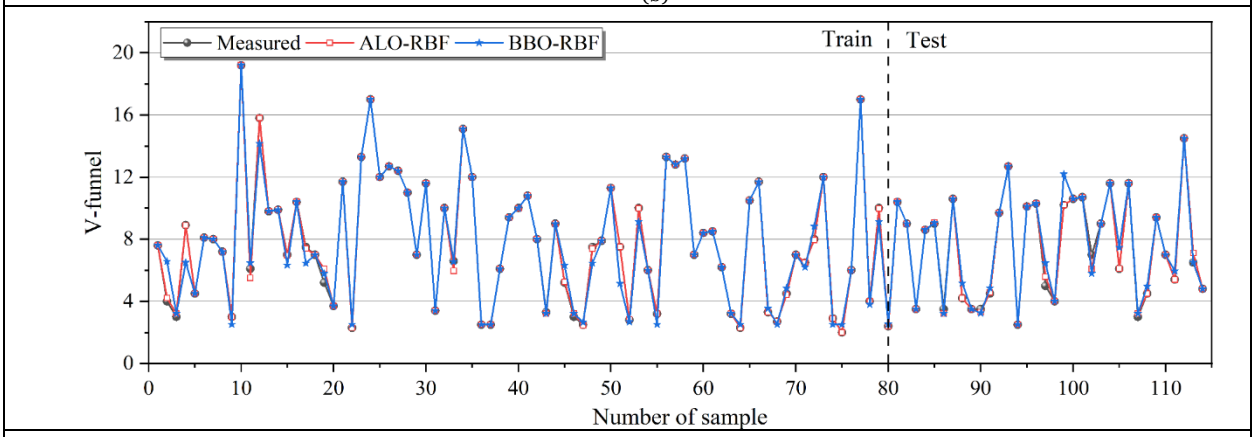

(c)

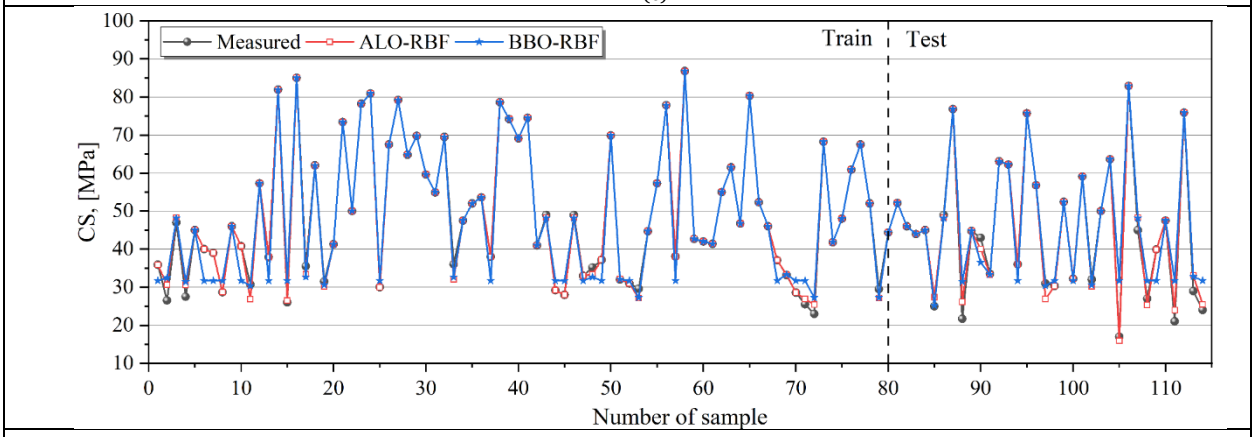

(d)

Fig. 7. Properties prediction using models for: a) D flow; b) L-Box; c) V-funnel; d) CS

4. Conclusion

It is received from the published articles that there were so limited studies concentrating on predicting either fresh or hardened properties of self-compacting concrete (SCC) using the optimized radial basis function neural network (RBFNN) method. Hence, it is tried to develop models for predicting the fresh and hardened properties of SCC by the RBFNN method. The RBFNN method has key parameters that can be optimized with optimization algorithms, where this study aimed to determine them using ant-lion optimization (ALO) and biogeography optimization (BBO) algorithms. The main results are as follows:

- Results demonstrate powerful potential in the learning section as well as approximating in the testing phase. It can be seen that the proposed models have R^2 in acceptable value in the learning and testing phase. It means that the correlation

between observed and predicted properties of SCC from hybrid models is acceptable so that it represents high accuracy in the training and approximating process.

- Regarding D flow, the results of ALO-RBFNN are so better than BBO-RBFNN as well as literature. For example, the RMSE value of the model by ALO in the training phase is 7.5154mm, while this value for the BBO-RBFNN model is more than twice, followed by Saha et al. (2020) at 11.67mm, and then Kaveh et al. (2018) by 36.29mm.
- Regarding L-box, the results of ALO-RBFNN are better than BBO-RBFNN as well as literature. For example, the RMSE value of the model by ALO in the testing phase is 0.0265, while this value for the BBO-RBFNN model is roughly less than twice, and followed by Saha et al. (2020) at 0.025, and then Kaveh et al. (2018) by 0.06.
- Turning to V-funnel results, the results of ALO-RBFNN are extremely better than BBO-RBFNN as well as literature. For instance, R^2 value of the model by ALO in the testing phase is 0.9951, while this value for BBO-RBFNN model is 0.9715, followed by Saha et al. (2020) at 0.958, and then Kaveh et al. (2018) by 0.87.
- Finally, the result for CS also depicts the same outputs as above. Overall, the RBFNN model developed by ALO outperforms others, which depicts the capability of the ALO algorithm for determining the optimal parameters of the considered method. However, it is worth mentioning that the model developed with the BBO algorithm is also powerful.
- For fresh and hardened properties of SCC in both optimized RBFNN (ALO-RBFNN and BBO-RBFNN) proposed models, the estimated values indicate suitable agreement with measured ones, expressing the workability of suggested integrated algorithms to forecast the D flow, L-box, V-funnel, and CS with high precision. According to time series figures, developed models result in the lowest variation in the properties predicting process, providing roughly accurate predictions which can be used for practical applications.

REFERENCES

[1] R. H. Faraj, A. A. Mohammed, and K. M. Omer, "Self-compacting concrete composites modified with nanoparticles: A comprehensive review, analysis and modeling," *J. Build. Eng.*, p. 104170, 2022.

[2] M. Benaicha, O. Jalbaud, A. H. Alaoui, and Y. Burtschell, "Porosity effects on rheological and mechanical behavior of self-compacting concrete," *J. Build. Eng.*, vol. 48, p. 103964, 2022.

[3] N. Hilal, T. A. Tawfik, S. N. Ahmed, and N. Hamah Sor, "The effect of waste medical radiology as fiber reinforcement on the behavior of eco-efficient self-compacting concrete," *Environ. Sci. Pollut. Res.*, pp. 1–14, 2022.

[4] A. Jain, S. Chaudhary, and R. Gupta, "Mechanical and microstructural characterization of fly ash blended self-compacting concrete containing granite waste," *Constr. Build. Mater.*, vol. 314, p. 125480, 2022.

[5] R. D. Saleh, N. Hilal, and N. H. Sor, "The Impact of a Large amount of Ultra-fine Sunflower Ash With/without Polypropylene Fiber on the Characteristics of Sustainable Self-compacting Concrete," *Iran. J. Sci. Technol. Trans. Civ. Eng.*, pp. 1–14, 2022.

[6] J. Wang, Q. Dai, and R. Si, "Experimental and Numerical Investigation of Fracture Behaviors of Steel Fiber–Reinforced Rubber Self-Compacting Concrete," *J. Mater. Civ. Eng.*, vol. 34, no. 1, p. 4021379, 2022.

[7] N. Garcia-Troncoso, L. Li, Q. Cheng, K. H. Mo, and T.-C. Ling, "Comparative study on the properties and high temperature resistance of self-compacting concrete with various types of recycled aggregates," *Case Stud. Constr. Mater.*, vol. 15, p. e00678, 2021.

[8] M. Esmaeili Falak, R. Sarkhani Benemaran, and R. Seifi, "Improvement of the Mechanical and Durability Parameters of Construction Concrete of the Qotursuyi Spa," *Concr. Res.*, vol. 13, no. 2, pp. 119–134, 2020, doi: 10.22124/JCR.2020.14518.1395.

[9] I. P. Sfikas, E. G. Badogiannis, and K. G. Trezos, "Rheology and mechanical characteristics of self-compacting concrete mixtures containing metakaolin," *Constr. Build. Mater.*, vol. 64, pp. 121–129, 2014.

[10] A. Beycioğlu and H. Y. Aruntaş, "Workability and mechanical properties of self-compacting concretes containing LLFA, GBFS and MC," *Constr. Build. Mater.*, vol. 73, pp. 626–635, 2014.

[11] B. Sukumar, K. Nagamani, and R. S. Raghavan, "Evaluation of strength at early ages of self-compacting concrete with high volume fly ash," *Constr. Build. Mater.*, vol. 22, no. 7, pp. 1394–1401, 2008.

[12] M. Jalal, A. Pouladkhan, O. F. Harandi, and D. Jafari, "Comparative study on effects of Class F fly ash, nano silica and silica fume on properties of high performance self compacting concrete," *Constr. Build. Mater.*, vol. 94, pp. 90–104, 2015.

[13] P. K. Acharya and S. K. Patro, "Effect of lime and ferrochrome ash (FA) as partial replacement of cement on strength, ultrasonic pulse velocity and permeability of concrete," *Constr. Build. Mater.*,

vol. 94, pp. 448–457, 2015.
[14] S.-W. Yoo, G.-S. Ryu, and J. F. Choo, “Evaluation of the effects of high-volume fly ash on the flexural behavior of reinforced concrete beams,” *Constr. Build. Mater.*, vol. 93, pp. 1132–1144, 2015.
[15] R. Sarkhani Benemaran, M. Esmaeili-Falak, and H. Katebi, “Physical and numerical modelling of pile-stabilised saturated layered slopes,” *Proc. Inst. Civ. Eng. Eng.*, pp. 1–16, 2020, doi: https://doi.org/10.1680/jgeen.20.00152.
[16] R. S. Benemaran and M. Esmaeili-Falak, “Optimization of cost and mechanical properties of concrete with admixtures using MARS and PSO,” *Comput. Concr.*, vol. 26, no. 4, pp. 309–316, 2020, doi: 10.12989/cac.2020.26.4.309.
[17] M. Esmaeili-Falak, H. Katebi, M. Vadiati, and J. Adamowski, “Predicting triaxial compressive strength and Young’s modulus of frozen sand using artificial intelligence methods,” *J. Cold Reg. Eng.*, vol. 33, no. 3, p. 4019007, 2019, doi: 10.1061/(ASCE)CR.1943-5495.0000188.
[18] A. Nassr, M. Esmaeili-Falak, H. Katebi, and A. Javadi, “A new approach to modeling the behavior of frozen soils,” *Eng. Geol.*, vol. 246, pp. 82–90, 2018, doi: 10.1016/j.enggeo.2018.09.018.
[19] F. Özcan, C. D. Atiş, O. Karahan, E. Uncuoğlu, and H. Tanyildizi, “Comparison of artificial neural network and fuzzy logic models for prediction of long-term compressive strength of silica fume concrete,” *Adv. Eng. Softw.*, vol. 40, no. 9, pp. 856–863, 2009.
[20] O. B. Douma, B. Boukhatem, M. Ghrici, and A. Tagnit-Hamou, “Prediction of properties of self-compacting concrete containing fly ash using artificial neural network,” *Neural Comput. Appl.*, vol. 28, no. 1, pp. 707–718, 2017.
[21] S. Kostić and D. Vasović, “Prediction model for compressive strength of basic concrete mixture using artificial neural networks,” *Neural Comput. Appl.*, vol. 26, no. 5, pp. 1005–1024, 2015.
[22] S. Subaşı, A. Beycioğlu, E. Sancak, and İ. Şahin, “Rule-based Mamdani type fuzzy logic model for the prediction of compressive strength of silica fume included concrete using non-destructive test results,” *Neural Comput. Appl.*, vol. 22, no. 6, pp. 1133–1139, 2013.
[23] R. Shadi and A. Nazari, “RETRACTED ARTICLE: Predicting the effects of nanoparticles on early age compressive strength of ash-based geopolymers by artificial neural networks,” *Neural Comput. Appl.*, vol. 31, pp. 743–750, 2019.
[24] M. Sonebi, A. Cevik, S. Grünewald, and J. Walraven, “Modelling the fresh properties of self-compacting concrete using support vector machine approach,” *Constr. Build. Mater.*, vol. 106, pp. 55–64, 2016.
[25] H. Y. Yang and Y. F. Dong, “Modelling concrete strength using support vector machines,” in *Applied Mechanics and Materials*, 2013, vol. 438, pp. 170–173.
[26] J. S. Yazdi, F. Kalantary, and H. S. Yazdi, “Prediction of elastic modulus of concrete using support vector committee method,” *J. Mater. Civ. Eng.*, vol. 25, no. 1, pp. 9–20, 2013.
[27] F. Naseri, F. Jafari, E. Mohseni, W. Tang, A. Feizbakhsh, and M. Khatibinia, “Experimental observations and SVM-based prediction of properties of polypropylene fibres reinforced self-compacting composites incorporating nano-CuO,” *Constr. Build. Mater.*, vol. 143, pp. 589–598, 2017.
[28] J. Liu, K. Yan, X. Zhao, and Y. Hu, “Prediction of autogenous shrinkage of concretes by support vector machine,” *Int. J. Pavement Res. Technol.*, vol. 9, no. 3, pp. 169–177, 2016.
[29] S. Yang, C. Q. Fang, and Z. J. Yuan, “Study on mechanical properties of corroded reinforced concrete using support vector machines,” in *Applied Mechanics and Materials*, 2014, vol. 578, pp. 1556–1561.
[30] A. Kaveh, T. Bakhshpoori, and S. M. Hamze-Ziabari, “M5’and Mars based prediction models for properties of self-compacting concrete containing fly ash,” *Period. Polytech. Civ. Eng.*, vol. 62, no. 2, pp. 281–294, 2018.
[31] P. Saha, P. Debnath, and P. Thomas, “Prediction of fresh and hardened properties of self-compacting concrete using support vector regression approach,” *Neural Comput. Appl.*, vol. 32, no. 12, pp. 7995–8010, 2020.
[32] I. Aljarah, H. Faris, S. Mirjalili, and N. Al-Madi, “Training radial basis function networks using biogeography-based optimizer,” *Neural Comput. Appl.*, vol. 29, no. 7, pp. 529–553, 2018.
[33] K. A. Rashedi, M. T. Ismail, N. N. Hamadneh, S. Wadi, J. J. Jaber, and M. Tahir, “Application of Radial Basis Function Neural Network Coupling Particle Swarm Optimization Algorithm to Classification of Saudi Arabia Stock Returns,” *J. Math.*, vol. 2021, 2021.
[34] X. Liu, X. Liu, Z. Zhou, and L. Hu, “An efficient multi-objective optimization method based on the adaptive approximation model of the radial basis function,” *Struct. Multidiscip. Optim.*, vol. 63, no. 3, pp. 1385–1403, 2021.
[35] M. Kasihmuddin, M. A. B. Mansor, S. A. Alzaeemi, and S. Sathasivam, “Satisfiability logic analysis via radial basis function neural network with artificial bee colony algorithm,” *Int. J. Interact. Multimed. Artif. Intell.*
[36] H. Wang *et al.*, “Image reconstruction for electrical impedance tomography using radial basis function neural network based on hybrid particle swarm optimization algorithm,” *IEEE Sens. J.*, vol. 21, no. 2, pp. 1926–1934, 2020.
[37] H.-G. Han, M.-L. Ma, H.-Y. Yang, and J.-F. Qiao, “Self-organizing radial basis function neural network using accelerated second-order learning algorithm,” *Neurocomputing*, vol. 469, pp. 1–12, 2022.

[38] H. Wu, Y. Han, Z. Geng, J. Fan, and W. Xu, "Production capacity assessment and carbon reduction of industrial processes based on novel radial basis function integrating multi-dimensional scaling," *Sustain. Energy Technol. Assessments*, vol. 49, p. 101734, 2022.

[39] E. M. Golafshani and G. Pazouki, "Predicting the compressive strength of self-compacting concrete containing fly ash using a hybrid artificial intelligence method," *Comput. Concr.*, vol. 22, no. 4, pp. 419–437, 2018.

[40] G. Pazouki, E. M. Golafshani, and A. Behnood, "Predicting the compressive strength of self-compacting concrete containing Class F fly ash using metaheuristic radial basis function neural network," *Struct. Concr.*, 2021.

[41] R. Siddique, P. Aggarwal, and Y. Aggarwal, "Influence of water/powder ratio on strength properties of self-compacting concrete containing coal fly ash and bottom ash," *Constr. Build. Mater.*, vol. 29, pp. 73–81, 2012.

[42] M. Şahmaran, İ. Ö. Yaman, and M. Tokyay, "Transport and mechanical properties of self consolidating concrete with high volume fly ash," *Cem. Concr. Compos.*, vol. 31, no. 2, pp. 99–106, 2009.

[43] S. Dhiyaneshwaran, P. Ramanathan, I. Baskar, and R. Venkatasubramani, "Study on durability characteristics of self-compacting concrete with fly ash," *Jordan J. Civ. Eng.*, vol. 7, no. 3, pp. 342–352, 2013.

[44] P. Muthupriya, P. N. Sri, M. P. Ramanathan, and R. Venkatasubramani, "Strength and workability character of self compacting concrete with GGBFS, FA and SF," *Int J Emerg Trends Eng Dev*, vol. 2, no. 2, pp. 424–434, 2012.

[45] B. Mahalingam and K. Nagamani, "Effect of processed fly ash on fresh and hardened properties of self compacting concrete," *Int J Earth Sci Eng*, vol. 4, no. 5, pp. 930–940, 2011.

[46] Y. Aggarwal and P. Aggarwal, "Prediction of compressive strength of SCC containing bottom ash using artificial neural networks," *Int. J. Math. Comput. Sci.*, vol. 5, no. 5, pp. 762–767, 2011.

[47] M. Uysal and K. Yilmaz, "Effect of mineral admixtures on properties of self-compacting concrete," *Cem. Concr. Compos.*, vol. 33, no. 7, pp. 771–776, 2011.

[48] R. Patel, "Development of statistical models to simulate and optimize self-consolidating concrete mixes incorporating high volumes of fly ash.," 2004.

[49] R. Gettu, J. Izquierdo, P. C. C. Gomes, and A. Josa, "Development of high-strength self-compacting concrete with fly ash: a four-step experimental methodology," in *Proc. 27th Conf. on Our World in Concrete & Structures, CI-Premier Pte. Ltd., Eds. CT Tam, DWS Ho, P. Paramasivam y TH Tan, Singapore*, 2002, pp. 217–224.

[50] E. Güneyisi, M. Gesoğlu, and E. Özbay, "Strength and drying shrinkage properties of self-compacting concretes incorporating multi-system blended mineral admixtures," *Constr. Build. Mater.*, vol. 24, no. 10, pp. 1878–1887, 2010.

[51] M. C. S. Nepomuceno, L. A. Pereira-de-Oliveira, and S. M. R. Lopes, "Methodology for the mix design of self-compacting concrete using different mineral additions in binary blends of powders," *Constr. Build. Mater.*, vol. 64, pp. 82–94, 2014.

[52] A. F. Bingöl and İ. Tohumcu, "Effects of different curing regimes on the compressive strength properties of self compacting concrete incorporating fly ash and silica fume," *Mater. Des.*, vol. 51, pp. 12–18, 2013.

[53] P. Krishnapal, R. K. Yadav, and C. Rajeev, "Strength characteristics of self compacting concrete containing fly ash," *Res J Eng Sci ISSN*, vol. 2278, p. 9472, 2013.

[54] P. Debnath and A. K. Dey, "Prediction of bearing capacity of geogrid-reinforced stone columns using support vector regression," *Int. J. Geomech.*, vol. 18, no. 2, p. 4017147, 2018.

[55] S. Mirjalili, "The ant lion optimizer," *Adv. Eng. Softw.*, vol. 83, pp. 80–98, 2015.

[56] D. Simon, "Biogeography-based optimization," *IEEE Trans. Evol. Comput.*, vol. 12, no. 6, pp. 702–713, 2008.

[57] W. Sun, D. Liu, J. Wen, and Z. Wu, "Modeling of MEMS gyroscope random errors based on grey model and RBF neural network," *J. Navig. Position*, vol. 5, pp. 9–13, 2017.

[58] S. Seshagiri and H. K. Khalil, "Output feedback control of nonlinear systems using RBF neural networks," *IEEE Trans. Neural Networks*, vol. 11, no. 1, pp. 69–79, 2000.